A new robot design for the interior exploration and inspection of pipe networks

Joonyoung Jang
Mechanical and Aerospace Engineering Department
University of California, San Diego
San Diego, USA
j7jang@ucsd.edu

Tao-Yi Wan

Mechanical and Aerospace Engineering Department
University of California, San Diego
San Diego, USA
twan@ucsd.edu

Thomas Bewley

Mechanical and Aerospace Engineering Department
University of California, San Diego
San Diego, USA
bewley@eng.ucsd.edu

Abstract—This research introduces a novel robot design for inspections, exploration, and mapping within complex pipe networks containing multiple curves and joints. The proposed pipe network inspection robot features four omniwheels in a single plane at the robot center, emphasizing simplicity, high maneuverability, and static stability. The robot is equipped with high torque motors capable of controlling roll motions. To enhance stability, the robot utilizes the spring-servo motor integrated series elastic actuator that maintains three or more points of contact with the opposite sidewalls of the pipe, causing the robot's center plane to align with the centerline of the pipe at all times during the operation. This design facilitates stable travel within the pipe at any orientation relative to gravity without requiring feedback. Furthermore, the robots are equipped with mechanisms for effectively navigating pipe curves and T-joints, as validated through hardware testing targeting roll control and maneuvering through pipe curves and joints.

Index Terms—in-pipe robot, pipe network inspection robot, series elastic actuator

I. Introduction

Pipe and duct networks are vital for global infrastructure, supplying water, natural gas, waste management, and building ventilation [1]. However, aging networks may cause leaks, causing the loss of valuable resources and releasing hazardous substances [2][3]. Thus, regular inspection and maintenance are essential to mitigate inefficiencies and protect the environment from potential damage. A substantial portion of these networks presents challenges for external access, as they are concealed underground, underwater, or within structures such as buildings, refineries, ships, or submarines. Furthermore, many older buried pipe systems lack accurate mapping, complicating their location and increasing the risk of damage during nearby construction or repair projects that involve extensive digging. To address these needs, pipe network inspection robots capable of internal inspection, exploration, and mapping play a vital role. These robots are designed to navigate intricate pipe networks characterized by bends, joints, diameter variations, and vertical sections, ensuring their reliable maneuverability.

There were many attempts to build efficient pipe network inspection robots. Snake or serpentine-style robots are typical designs for pipe network inspection [4][5][6]. However, these robots are typically long, complex, and have high blockage. Snake robots are driven by multiple treads or wheels around their circumference that can be pushed outward to grip the pipe wall. These robots are usually assembled into multiple independent modules incorporating many different motors for articulation and locomotion. One of the pioneering snake robot designs was Explorer II; snake robots of this general overall design target a variety of pipe diameters [7]. Another type of robot for pipe network inspection is a screw drive in-pipe robot. These robots use two large rotating screws to propel themselves through the pipe [8][9]. This design is hard to negotiate curves or joints. Some designs have six or more wheels mounted on spring-loaded arms about the robot core [10]. Half of these arms are attached to one end of the vehicle and half to the other; each folds outward from the body of the vehicle as necessary to grip the walls, allowing the robot to handle pipes of various diameters. Such robots are more complex and have higher blockage. There are rover-type designs deployed within large mainline pipes but generally cannot maneuver controllably into pipe branches at joints in pipe networks. Such robots include one or more arms that can push one or more wheels against the opposite side of the pipe for added stability during roll [11][12]. The closest existing robot design to the robot proposed in this paper is a tethered W-shaped design with pairs of omniwheels acting together as drive wheels at each of the three interior joints and pairs of half-spherical wheels at each end acting as control wheels [13]. Compared to the W-shaped design, named AIRo-II, our designs are less complex, with fewer wheels and lower blockage. Also, AIRo-II design does not incorporate Series Elastic Actuators(SEA), with springs, to inherently obtain stability by passively expanding the robot across the full breadth of the pipe over different diameters, with the springs firmly pressing the wheels against opposite walls at least three

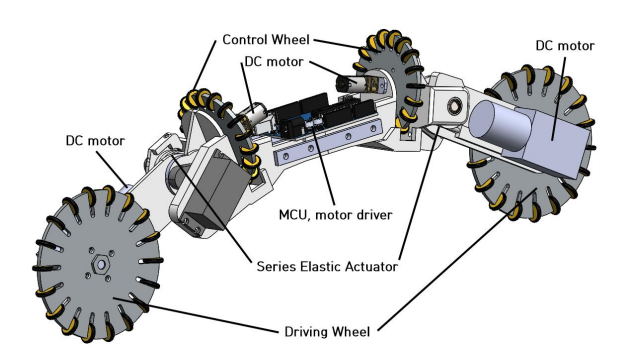


Fig. 1: The overall configuration of the proposed pipe network inspection robot.

alternating points of contact at all times. The roll control in the AIRo-II design is achieved with two sets of spherical wheels instead of driving two orthogonally arranged omniwheels used in the proposed robot.

The paper is organized as follows. Section II presents the design and hardware properties of the robot. Section III discusses static analysis to obtain the required motor torques essential for choosing actuators. In Section IV, the hardware tests, including roll control and T-joint maneuvering, were performed to test the mobility of the robot inside the pipeline. Section V suggests future works to improve robot performance and develop control algorithms for autonomous robot navigation.

II. DESIGN

A. Mechanical Design

The robot design aims to operate inside a pipe, including T-joints and curves. Fig. 1 shows the overall configuration of the robot. This design has two robot arms with two omniwheels driven by high torque worm gear dc motors. These are 'Driving wheels' that maneuver a robot forward and backward. Robot arms are connected with a body frame via Series Elastic Actuators(SEAs). The SEA mechanical system discussed in II-B can exert continuous forces on the pipe wall to stabilize pitch and yaw motions during operations regardless of the direction of gravity, even when maneuvering through complex networks of connected pipes with pipe curves, joints, and significant pipe diameter changes.

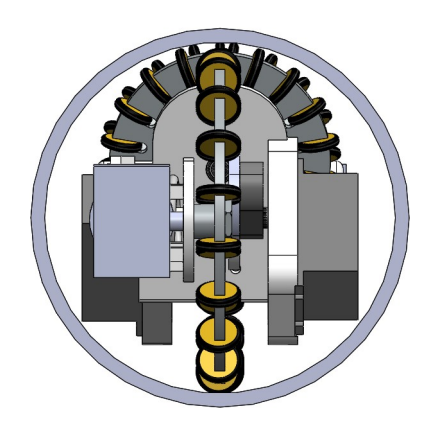
There are two omniwheels attached to the body frame. These wheels are 'Control wheels' driven by geared dc motors and can control a robot's roll motion since they are vertical to the pipe axial center line. The robot mainly aims to operate inside a 4-inch pipe. All hardware parts are selected and designed to fit a 4-inch diameter pipe, as seen in Fig. 2.

B. Series Elastic Actuator

The Series Elastic Actuator (SEA) is a mechanism known for reducing the stiffness of actuators, thus removing the risk of applying unintentional forces directly to motor components [14]. SEAs can transmit force or torque to connected mechanisms by deflecting elastic materials, eliminating the need



(a) Front-view.



(b) End-view.

Fig. 2: Robot inside a 4-inch diameter pipe

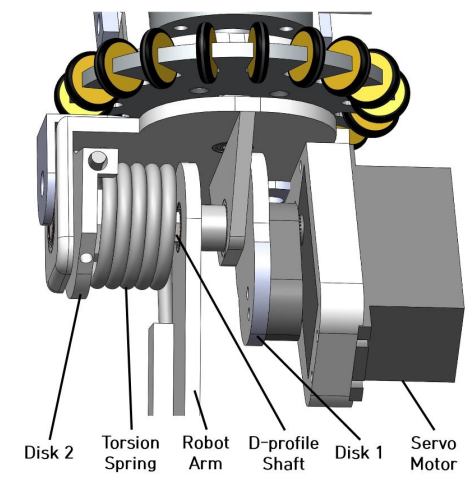


Fig. 3: Series Elastic Actuator(SEA) applied to shoulders of the robot.

for extra motor actuation [15]. Fig. 3 illustrates the SEA mechanism applied in the robot. It consists of a servo motor connected to Disk 1, which is linked to the D-profile shaft. The D-profile shaft passes through a bearing on a robot arm, connecting Disk 1 and Disk 2. A torsion spring connects Disk 2 to the robot arm. When the robot arm comes into contact with the pipe wall and cannot rotate further, the torsion spring deflects as the robot arm is freely rotated from the shaft. The deflection loads a torsion spring, exerting continuous forces applied to the pipe walls.

TABLE I: Prototype Hardware Lists

Hardware	Supplier	Model
DC motor(Driving)	Yosoo	12V 10RPM Worm gear motor
DC motor(Control)	Greartisan	12V 78RPM gear motor
Servo motor	Sincecam	40kg High Torque Servo
Omniwheel(Driving)	GTF Robots	100mm Aluminum Omniwheel
Omniwheel(Control)	GTF Robots	70mm Aluminum Omniwheel
Torsion spring	Mcmaster	9271K592
SEA Shaft	Robot shop	6mm D Shaft
Bearing	Mcmaster	57155K585, 7804K141
Microprocessor	Arduino	Uno
Motor controller	Pololu	TB6612FNG
Power Supply	AlloverPower	3-24V DC Power Supply Kit

^{*} Body frame, Robot arm, SEA Disk 2 are 3D printed, and SEA Disk 1 is laser cut aluminum.

C. Hardware

The prototype of the robot was built using a 3D-printed body frame manufactured with Formlabs' Rigid 4000 resin, known for its durability, heat resistance, and stability [16]. This prototype incorporates SEAs comprising a torsion spring, high-torque low-profile servo motor, D-profile shaft, 3Dprinted and laser-cut D-profile Disks, and a robot arm. The servo motor has a maximum torque capacity of 3922.66mNm, sufficient to handle the deflection and loading of the torsion spring with a maximum torque of 3163.58mNm. The Driving wheel dc motors are worm gear motors with a rated torque of 980.67mNm, and the Control wheel DC motors are geared motors with a rated torque of 196.13mNm. All motors are controlled by an Arduino Uno microprocessor and TB6612FNG dual motor driver. The robot features 100mm(3.93inches) diameter omniwheels for driving wheels and 70mm (2.76 inches) diameter for control wheels. Their centers are aligned with the pipe's axial plane. Dc motors actuate omniwheels to control forward, backward, and roll motions. Table I lists the hardware components used to build the robot.

III. STATIC ANALYSIS

Studying the statics of our robot provides insight into the required forces to maintain a stable pose and maneuver inside the pipe. Also, statics is essential for choosing hardware parts, especially motors providing required torques.

A. Driving Wheel and Servo Motor Torques

Fig. 4 is the free-body diagram of the front view inside a tilted 4-inch pipe. The statics parameters are listed in Table II. r_d and r_c represent the driving and control wheel radius. d is the arm length from the SEA shaft center, and l is the body length representing the distance between two Control wheel centers. n is the length between the Control wheel and SEA shaft centers. The angles α_1 , α_2 are the arm angles, while β_1 , β_2 are the Control wheel angles. As the pipe tile angle is θ , gravitational forces can be written as $mq\sin\theta$, and $mq\cos\theta$

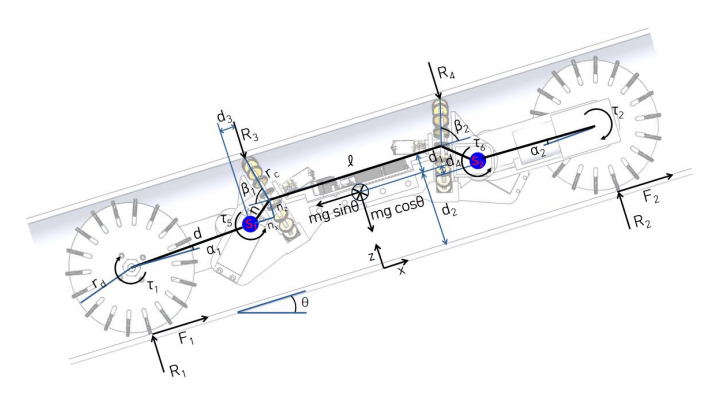


Fig. 4: Free-Body Diagram(Front-view): To compute the required Driving wheel and SEA torques for driving a robot and maintaining the stable pose inside the tilted pipe with pitch angle θ .

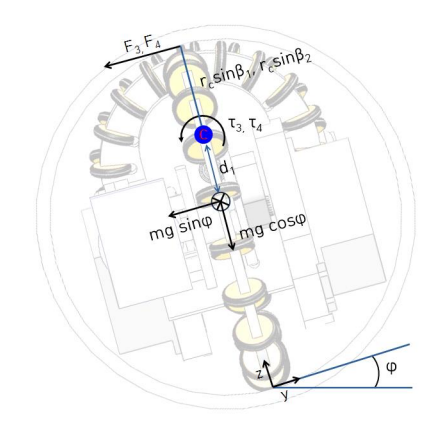


Fig. 5: Free-Body Diagram(End-view): To compute the required Control wheel torques for the roll control with roll angle ϕ .

TABLE II: Statics Parameters

Categories	Parameters	Magnitude
Driving wheel radius	r_d	50.00mm
Control wheel radius	r_c	35.00mm
Arm length	d	92.18mm
Body frame length	l	135.50mm
SEA distance	$n(n_x, n_z)$	22.92mm, 16.09mm
Arm angle	α_1, α_2	0.63° (4 inch pipe)
Control wheel angle	β_1, β_2	75°
Total mass	m	950g
Distance	$d_1, d_2,$	13.87mm, 53.93mm,
	d_{3}, d_{4}	15.32mm, 2.96mm
Roll, Pitch, Yaw	ϕ, θ, ψ	-
Wheel force	F_1, F_2, F_3, F_4	-
Wheel torque	$ au_{1}, au_{2}, au_{3}, au_{4}$	-
SEA torque	$ au_5, au_6$	-
Reaction force	R_1, R_2, R_3, R_4	-

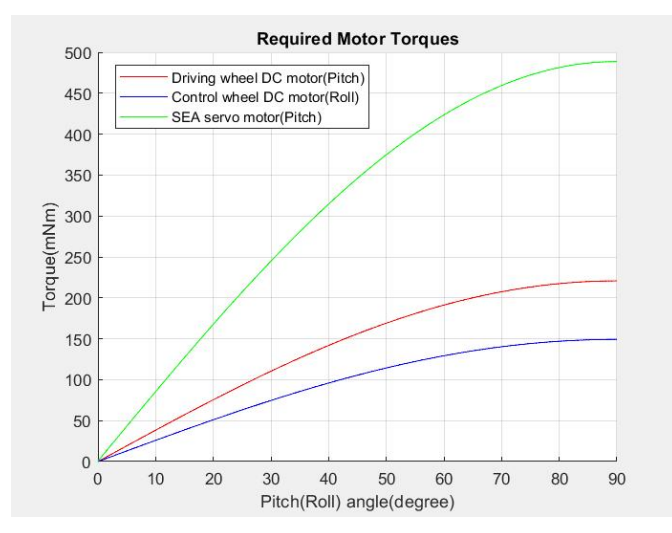


Fig. 6: Required motor torques about pitch (roll) angle.

in x, z axis. By Newton-Euler equations, the sum of forces and torques at the static equilibrium can be written as follows,

$$\sum F_x : F_1 + F_2 = mg \sin \theta,$$

$$\sum F_z : R_1 + R_2 = R_3 + R_4 + mg \cos \theta,$$

$$\sum \tau_w : \tau_1 + \tau_2 = r_d F_1 + r_d F_2,$$

$$\sum \tau_{s1} : \tau_5 = -F_1 (d \sin \alpha_1 + r_d) - R_1 (d \cos \alpha_1)$$

$$- d_3 R_3 - (n_x + \frac{l}{2}) \frac{mg \cos \theta}{2} + d_4 \frac{mg \sin \theta}{2},$$

$$\sum \tau_{s2} : \tau_6 = -F_2 (d \sin \alpha_2 + r_d) - R_2 (d \cos \alpha_2)$$

$$- d_3 R_4 - (n_x + \frac{l}{2}) \frac{mg \cos \theta}{2} + d_4 \frac{mg \sin \theta}{2},$$

$$\sum \tau_b : R_1 (\frac{l}{2} + n_x + d \cos \alpha_1) = R_3 (\frac{l}{2} + r_c \cos \beta_1) + d_2 F_1,$$
(1)

with F_1 and F_2 are the forces moves a robot forward, and R_1 , R_2 , R_3 , and R_4 are reaction forces on the wheels. τ_w , τ_{s1} and τ_{s2} relatively represent the required torques of the Driving wheel DC motor and SEA servo motors. τ_b is the sum of torque at the mass center located in the middle of the body frame. Assuming that control wheel($\beta_1 = \beta_2$) and arm angles($\alpha_1 = \alpha_2$), forces($F_1 = F_2$), and torques($\tau_1 = \tau_2$, $\tau_{s1} = \tau_{s2}$) of left and right halves are equivalent, (1) can be simplified and solved for driving wheel torque τ_w and SEA servo motor torque τ_s ,

$$\begin{split} \tau_w &= \frac{r_d mg \sin \theta}{2}, \\ \tau_s &= c_1 R_1 + d_3 R_3 + c_2 F + c_3 \frac{mg \cos \theta}{2} - d_4 \frac{mg \sin \theta}{2}, \end{split} \tag{2}$$
 with constants defined as,

$$c_1 = d\cos\alpha, \quad c_2 = d\sin\alpha + r_d, \quad c_3 = n_x + \frac{l}{2},$$

 $c_4 = \frac{l}{2} + n_x + d\cos\alpha, \quad c_5 = \frac{l}{2} + r_c\cos\beta$

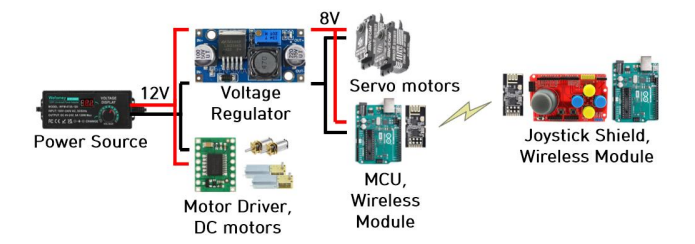


Fig. 7: Electonics setup for the prototype robot control.

and the reaction forces can be written as follows,

$$R_1 = \frac{c_5 mg \cos \theta - 2d_2 F}{2(c_5 - c_4)}, \quad R_3 = \frac{c_4 R_1 - d_2 F}{c_5}.$$

Fig. 6 shows the required motor torques computed by (2). Required DC motor torques τ_w vary about the pipe tilt angle θ . The maximum required torque for climbing the vertical pipe was 220.73mNm. τ_s changes as the pipe tilt angle varies. Inside the 4-inch pipe, the arm angles are fixed as 0.63° . Thus, τ_s is the function of θ , and Fig. 6 is the required SEA torque to maintain the robot pose inside the pipe depending on the pipe tilt angle. The maximum τ_s is when the pipe is vertical, which was 488.66mNm.

B. Control Wheel Torque

Fig. 5 is the free body diagram of the end-view. As the robot rolls with an angle ϕ , the sum of forces and the torque on the Control wheel center can be written as,

$$\sum F_y : F_3 + F_4 = mg\sin\phi,\tag{3}$$

$$\sum \tau_c : \tau_3 + \tau_4 = F_3 r_c \sin \beta_1 + F_4 r_c \sin \beta_2. \tag{4}$$

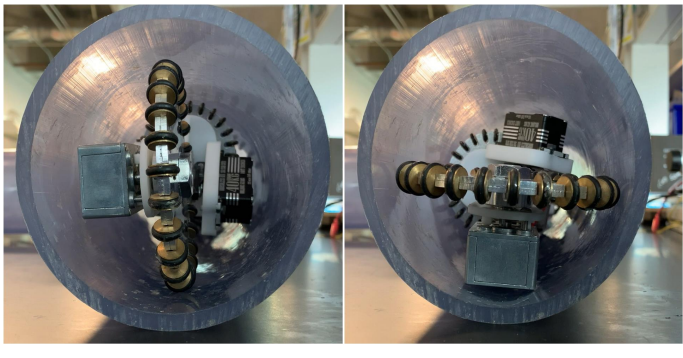
 au_c represents the required torque of the Control wheel motor. Assuming that both the Control wheels' forces($F_3=F_4$) and torques($au_3= au_4$) are the same, then (4) can be rewritten about control wheel torque au_c ,

$$\tau_c = \frac{(r_c \sin \beta) mg \sin \phi}{2}.$$
 (5)

As (5) is the function of the roll angle ϕ , the required torque varies as shown in Fig. 6. The maximum required torque was 149.24mNm when the roll angle was 90°.

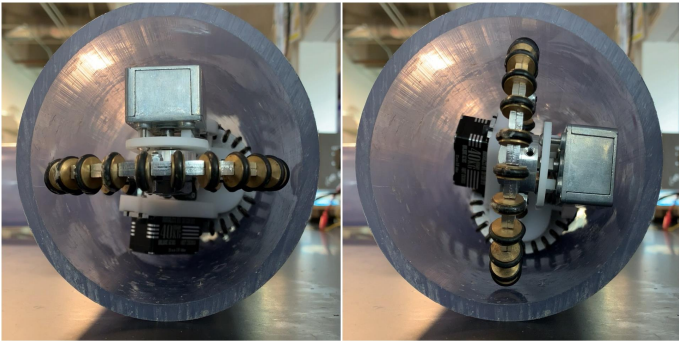
IV. EXPERIMENT

The prototype robot is manually controlled by an operator, and the electronics setup is as shown in Fig. 7. The power source provides 12-voltage power to the motor driver(TB6612FNG) and dc motors. A voltage regulator(LM2596) converts power to 8-voltage for servo motors and a microprocessor. A wireless module(NRF24L01) allows wireless communication with the Arduino joystick shield. The joystick can control the forward-backward motions, roll, and arm angles.



(a) 0° Roll.

(b) 90° Counter clock wise.



(c) 90° Clock wise.

(d) 180° Roll.

Fig. 8: Roll motion test inside the 4-inch pipe.

A. Roll Motion

A roll control test was performed inside the 4-inch diameter horizontal pipe. Since control wheels are orthogonally installed to the body and driven by geared motors, the robot can roll by actuating control wheel motors. As seen in III-A, each motor's required torque for the roll control is a maximum of 149.24mNm at 90° roll angle. A control wheel motor has 193.13mNm rated torque, providing enough torque to control the roll of a robot at any angle. In Fig. 8, the roll motion test inside the pipe was done with chosen motors, and the results showed that the robot could roll in both directions to 90° and 180° angles. SEAs generate continuous pushing forces against the wall so that the robot can maintain stability during the roll test. The roll test experiment video was posted to the following link: https://youtu.be/sGsYZAuReSo

B. Curve Maneuver

The complex pipe networks consist of angled curves along with straight pipes. Fig. 9a shows the robot inside the 4-inch diameter curve. As the robot reached the curve, the robot kept moving forward and pushed the rear robot arm to the pipe wall by changing the rear arm angle. As the robot passes the corner of the curve, actuate the Control wheels to roll until the robot's pose is straight up. This prevents the robot stuck inside the corner and ensure smoothly passes curve and proceed to the next pipeline. The curve maneuver test experiment video was posted to the following link: https://youtu.be/iuFPbDE0UfY

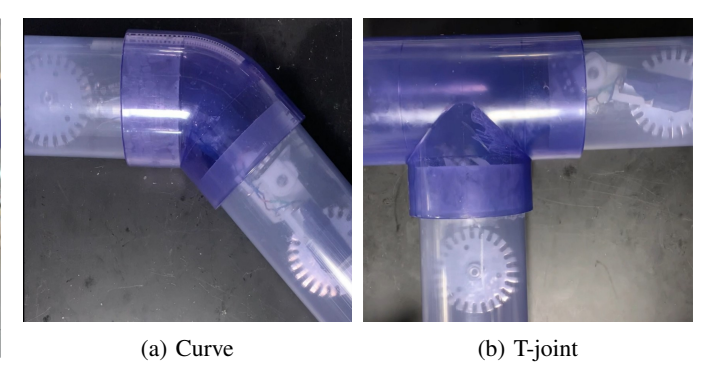


Fig. 9: The robot inside the curve and T-joint.

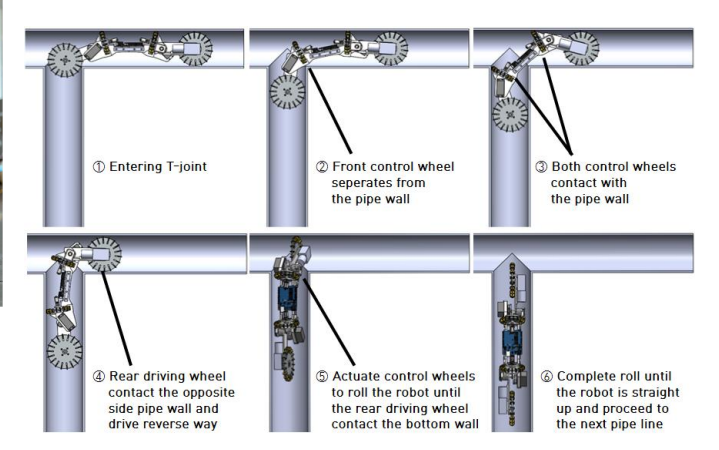


Fig. 10: 4-inch diameter T-joint pipe maneuvering.

C. T-joint Maneuver

Fig. 9b shows the robot inside the 4-inch diameter T-joint. The strategy of the T-joint maneuvering is illustrated in Fig. 10. As SEAs provide continuous grabbing forces to the robot arms against the pipe wall, at least three wheels maintain contact with the wall while turning a T-joint. As the front Driving wheel goes into the joint when the robot enters the T-joint, the front Control wheel separates from the pipe wall. Arm angles are adjusted by actuating SEA servo motors to maintain the grabbing forces and the stable pose until the front Control wheel attaches to the next pipeline wall. At this point, by changing the arm angle, the rear driving wheel contacts the opposite side pipe wall. As the rear driving wheel contacts the pipe wall, actuate the rear driving wheel in the reverse direction to facilitate pushing force for moving the robot forward. Continuing maneuvering the robot to the next pipeline, the rear driving wheel slips at the corner of the Tjoint. To overcome the slippage, actuate the Control wheels to roll the robot until the rear driving wheel contacts the bottom pipe wall, and simultaneously actuate the Driving wheels forward. Complete the roll until the robot is straight up and proceed to the next pipeline. The T-joint experiment video was posted to the following link: https://youtu.be/SQVwASIToo4

V. CONCLUSION

In this paper, we proposed a novel pipe network inspection robot design targeting the operation inside the 4-inch pipe. The robot has four omniwheels driven by DC motors. Two wheels control the robot's forward and backward motions and other wheels are aligned orthogonally to the body center line for roll control. Also, a torsion spring and a servo motor embedded SEA allows changing the robot arm angles, providing continuous force against the pipe wall during operation. especially when turning the curves or T-joints. The static analysis gives insight into the required torques of DC motors and SEA servo motors essential for choosing hardware parts. The tests were performed to verify the mobility of the proposed mechanical design inside the pipeline curves and joints. The result proved that the proposed robot passes through curves and a T-joint, showing the ability of the robot to explore the complex pipeline. Future works focus on developing the autonomous navigation control algorithm for operation inside the pipeline. The feedback control system is essential for autonomous navigation, utilizing an IMU sensor to maintain a stable pose during the operation and pass through curves and T-joints. Since the robot uses battery power, the algorithm aims for energy-efficient operation, exploring all pipelines with the minimum travel distance. Further, pipe damage detection utilizing the camera vision and will be studied and applied in future models.

ACKNOWLEDGMENT

The authors gratefully acknowledge financial support of the ERDC Construction Engineering Research Laboratory (CERL) via a subcontract with GTI Energy. The authors also thank Zachary Hooker and Pablo Tejeda for related work on earlier versions of these designs.

REFERENCES

- [1] C. Zou, Z. Yang, D. He, Y. Wei, J. Li, A. Jia, J. Chen, Q. Zhao, Y. Li, J. Li, S. Yang, "Theory, technology and prospects of conventional and unconventional natural gas," Petroleum Exploration and Development, Volume 45, Issue 4, 2018, pp. 604-618, ISSN 1876-3804, https://doi.org/10.1016/S1876-3804(18)30066-1.
- [2] S. Nešić, "Key issues related to modelling of internal corrosion of oil and gas pipelines A review," Corrosion Science, Volume 49, Issue 12, 2007, pp. 4308-4338, ISSN 0010-938X, https://doi.org/10.1016/j.corsci.2007.06.006.
- [3] R. Parkins, "A Review of Stress Corrosion Cracking of High Pressure Gas Pipelines." Paper presented at the CORROSION 2000, Orlando, Florida, March 2000.
- [4] S. D. Nivethika, T. Nivethetha, P. Priyadharshini, V. T. Nithyasri, M. SenthilPandian and R. Sivaprasad, "Design and Development of Pipe inspection Snake Locomotion Robot," 2022 International Conference on Power, Energy, Control and Transmission Systems (ICPECTS), Chennai, India, 2022, pp. 1-5, doi: 10.1109/ICPECTS56089.2022.10047028.
- [5] C-W. Huang, C-H. Huang, Y. Hung, and C. Chang, "Sensing pipes of a nuclear power mechanism using low-cost snake robot," Advances in Mechanical Engineering, 2018, 10(6), doi:10.1177/1687814018781286.
- [6] T. Kamegawa, T. Baba and A. Gofuku, "V-shift control for snake robot moving the inside of a pipe with helical rolling motion," 2011 IEEE International Symposium on Safety, Security, and Rescue Robotics, Kyoto, Japan, 2011, pp. 1-6, doi: 10.1109/SSRR.2011.6106789.
- [7] S. Burkett, and H. Schempf, "Wireless Self-powered Visual and NDE Robotic Inspection System for Live Gas Distribution Mains," United States: N. p., 2006, Web, doi:10.2172/876616.

- [8] T. Li, S. Ma, B. Li, M. Wang and Y. Wang, "Design of spring parameters for a screw drive in-pipe robot based on energy consumption model," Proceeding of the 11th World Congress on Intelligent Control and Automation, Shenyang, China, 2014, pp. 3292-3297, doi: 10.1109/WCICA.2014.7053260.
- [9] H. Tourajizadeh and M. Rezaei, "Design and control of a steerable screw in-pipe inspection robot," 2016 4th International Conference on Robotics and Mechatronics (ICROM), Tehran, Iran, 2016, pp. 98-104, doi: 10.1109/ICROM.2016.7886824.
- [10] J. Min, Y. Liauw, P. Pratama, S. Kim, H. Kim, "Development and Controller Design of Wheeled- Type Pipe Inspection Robot," Proceedings of the 2014 International Conference on Advances in Computing, Communications and Informatics, ICACCI 2014, 10.1109/ICACCI.2014.6968543.
- [11] Y. Kwon, E. Jung, H. Lim, B. Yi, "Design of a reconfigurable indoor pipeline inspection robot", Control, Automation and Systems, 2007, ICCAS '07, International Conference on, pp. 712-716, doi: 10.1109/IC-CAS.2007.4406991.
- [12] J. Knedlová, O. Bílek, D. Sámek, P. Chalupa, "Design and construction of an inspection robot for the sewage pipes," MATEC Web of Conferences, 2017, doi: 10.1051/matecconf/20171210100610.1051/matecconf/201712101006.
- [13] A. Kakogawa and S. Ma, "Design of a multilink-articulated wheeled inspection robot for winding pipelines: AIRo-II," 2016 IEEE/RSJ International Conference on Intelligent Robots and Systems (IROS), Daejeon, Korea (South), 2016, pp. 2115-2121, doi: 10.1109/IROS.2016.7759332.
- [14] K. D. Truong, A. K. L. Luu, N. P. Tong, V. T. Duong, H. H. Nguyen and T. T. Nguyen, "Design of Series Elastic Actuator Applied for Humanoid," 2020 International Conference on Advanced Mechatronic Systems (ICAMechS), Hanoi, Vietnam, 2020, pp. 23-28, doi: 10.1109/ICAMechS49982.2020.9310118.
- [15] J. Jang et al., "Design and Characterization of the Torsion Spring-Motor Integrated Series Elastic Actuator," 2023, Manuscript submitted for publication.
- [16] Formlabs, "Rigid 4000 Resin for Stiff, Strong, Engineering-Grade Prototypes," accessed 22 August 2023, https://formlabs-media.formlabs.com/datasheets/1801088-TDS-ENUS-0.pdf